AIP Journal of Applied Physics

Adjusting exchange bias and coercivity of magnetic layered systems with varying anisotropies

A. Ehrmann née Tillmanns and T. Blachowicz

Citation: J. Appl. Phys. 109, 083923 (2011); doi: 10.1063/1.3575170
View online: http://dx.doi.org/10.1063/1.3575170
View Table of Contents: http://jap.aip.org/resource/1/JAPIAU/v109/i8
Published by the American Institute of Physics.

JOURNAL OF APPLIED PHYSICS **109**, 083923 (2011)

Adjusting exchange bias and coercivity of magnetic layered systems with varying anisotropies

A. Ehrmann née Tillmanns[1,a)] and T. Blachowicz[2]
[1]*FTB, Niederrhein University of Applied Sciences, 41065 Mönchengladbach, Germany*
[2]*Institute of Physics, Silesian University of Technology, 44-100 Gliwice, Poland*

(Received 1 February 2011; accepted 15 March 2011; published online 21 April 2011)

The impact of a variation of anisotropy constants on the resulting coercivity and exchange bias has been analyzed modeling the total energy density in thin layered ferromagnetic/antiferromagnetic in-plane systems. For a broad range of fourfold, uniaxial, and unidirectional anisotropies, our results illustrate that the exchange bias can grow significantly for a sample rotation off the cooling field direction, while for other combinations of anisotropies, a positive exchange bias can be found near or even in the cooling field direction. These findings allow identification of anisotropies based on superconducting quantum interference device or magneto-optical Kerr effect measurements as well as tailoring desired angular dependencies for magnetoelectronic applications. © *2011 American Institute of Physics*. [doi:10.1063/1.3575170]

I. INTRODUCTION

A magnetic system composed of an antiferromagnetic (AFM) and a ferromagnetic (FM) layer can exhibit a shift of the hysteresis loop along the field axis, the so-called exchange bias (EB).[1–3] This effect can be observed when the system is cooled below the Néel temperature of the AFM in an external magnetic field.

The EB can, along with other magnetic anisotropies, influence the measured angular dependence of the coercivity. An established optical method for quantitatively determining magnetic anisotropies by measurements of anisotropy constants is, for example, Brillouin light scattering.[4] However, as has been shown in a previous article for samples without exchange bias,[5] measurements of the coercivity by means of the magneto-optic Kerr effect (MOKE) also enable the determination of the anisotropy constants of a magnetic sample. Thus, in this article we provide an overview of the effects of changes in the fourfold, uniaxial, and unidirectional anisotropy constants of magnetic layers on angular dependent coercivity and exchange bias. This comprehensive study provides the possibility of an estimate of a sample's anisotropies based on the results of MOKE or superconducting quantum interference device measurements. On the other hand, it also gives the possibility to tailor desired angular dependencies of exchange bias and coercivity by choosing materials or geometries with the respective anisotropies for specific applications. Finally, it provides a novel explanation for the positive exchange bias and the theoretical base which has frequently been discussed in the literature.[6–8] This effect has been attributed to a parallel coupling of FM and AFM moments at the interface due to large cooling fields,[9–11] antiferromagnetic coupling at the interface,[12–15] a mainly antiferromagnetic parallel domain wall which is "unwinding" before zero field,[16] spin-glass-like particles formed spontaneously at the interface,[17] or to reversible changes in the interfacial pinning by the antiferromagnet causing an asymmetric magnetization reversal.[18] What is proposed here, however, is the simple possibility to obtain positive exchange bias in a special EB system without the need to consider directly any effects on an atomic scale.

II. MODELING ANISOTROPIES

In our systematic study, we use a simple model describing the coherent rotation of a magnetic moment or macrospin. It allows the determination of coercive fields from magnetic anisotropies.

In the recent literature, exchange bias systems with polycrystalline layers are mostly examined.[19–22] However, epitaxial or textured samples may exhibit interesting and sometimes quite unexpected findings. In the system Fe/MnF_2(110) with a twinned antiferromagnet, e.g., an asymmetric hysteresis loop has been found at low temperatures.[23–27] Asymmetric magnetization reversal has also been found in Fe/FeF_2(110) with twinned AFM.[25,28–31] Simulations assuming a twinned antiferromagnet by introducing two easy axes in the AFM perpendicular to each other also led to asymmetric hysteresis loops.[32] On the other hand, systems with uniaxial and fourfold anisotropy, like Co/CoO(110), may exhibit an exchange of the hard and the easy axis in a temperature regime around the blocking temperature[33] and thus lead to interesting effects in the transition region.

Due to the importance in fundamental research of such systems with uniaxial and fourfold anisotropy, combined with an exchange bias, our study focuses on this special type of magnetic system. Thus, the following expression for the free energy density of the FM layer is used:

$$F_{\mathrm{ani}}(\phi) = K_{||}^{(4)} \cos^2(\phi)\sin^2(\phi)\sin^4(\theta) + K_{||}^{(2)} \cos^2(\phi)\sin^2(\theta) + K_{||}^{(1)} \cos(\phi - \phi_{\mathrm{EB}})\sin(\theta) \quad (1)$$

[a)]Author to whom correspondence should be addressed. Electronic mail: andrea.ehrmann@hsnr.de.

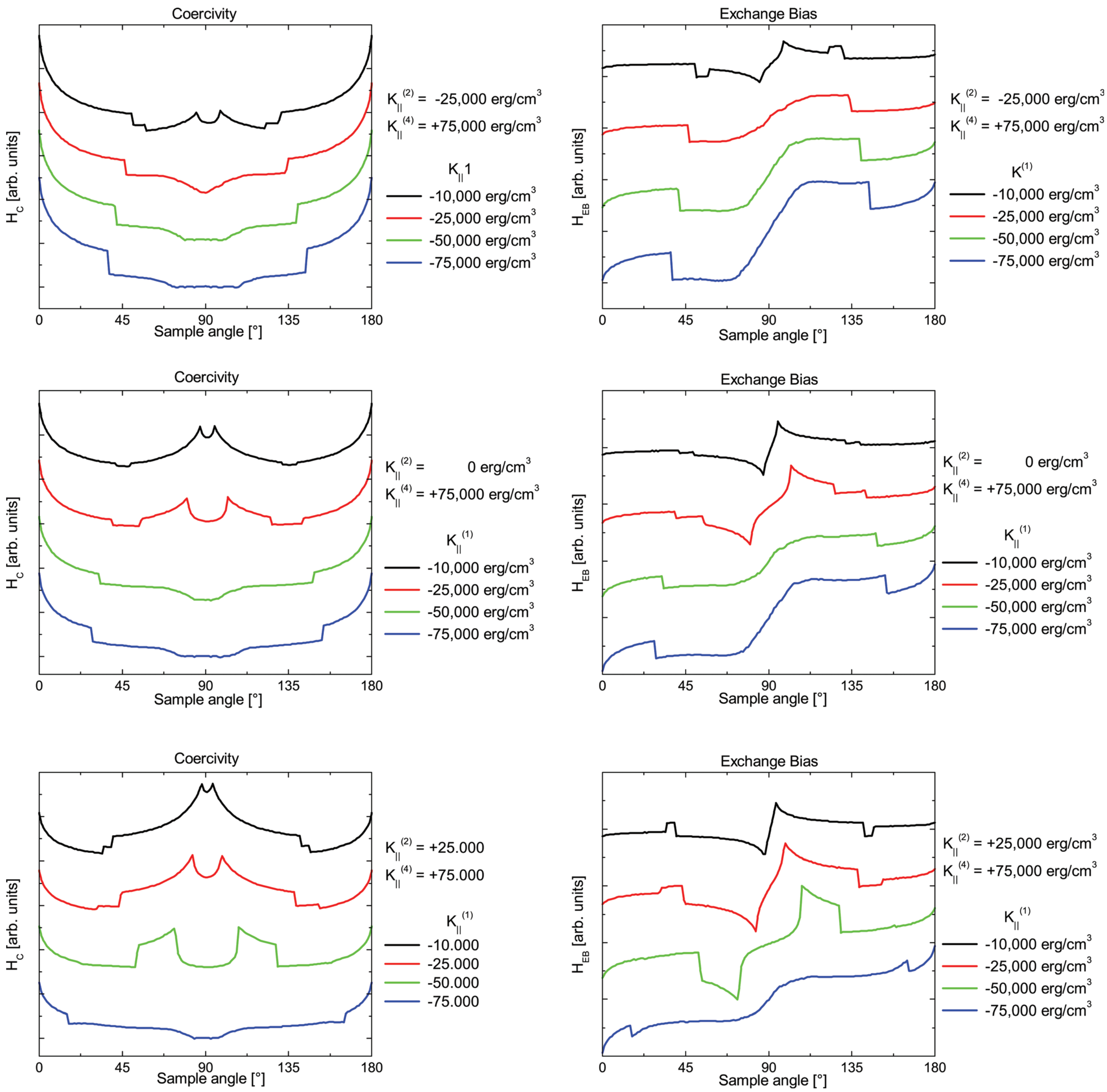

FIG. 1. (Color online) Exchange bias and coercivity calculated for a series of unidirectional anisotropies $K_{||}^{(1)}$ (with the values increasing numerically from top to bottom), for $K_{||}^{(4)} = 75\,000$ erg/cm^3 and $K_{||}^{(2)} = -25\,000$ erg/cm^3 (upper panels)/0 erg/cm^3 (middle panels)/+ 25 000 erg/cm^3 (lower panels). Lines are vertically shifted for clarity.

and its first derivative (assuming the in-plane case, thus $\theta = 90°$)

$$\frac{\partial F_{\mathrm{ani}}(\phi)}{\partial \phi} = (1/2)K_{||}^{(4)}\sin(4\phi) - K_{||}^{(2)}\sin(2\phi) - K_{||}^{(1)}\sin(\phi - \phi_{\mathrm{EB}}) \quad (2)$$

where ϕ is the in-plane sample orientation angle with respect to the magnetic field direction; θ is the angle between the surface normal and the magnetization vector direction; ϕ_{EB} is the easy exchange bias direction; and $K_{||}^{(4)}$, $K_{||}^{(2)}$, and $K_{||}^{(1)}$ are the anisotropy constants of the fourth, second, and first (exchange bias) order, respectively.[33] The exclusions of perpendicular anisotropies in Eqs. (1) and (2) result from the assumption that no interfacial alloying or strains or interfacial magnetostriction effects take place in the discussed systems.

The coercive fields are calculated by identifying the external field which is sufficient to switch the magnetization over the transverse state (perpendicular to the magnetic field). For this purpose, the first derivation of the free energy density [Eq. (2)] is used: As soon as the free energy density decreases continuously from saturation magnetization to a

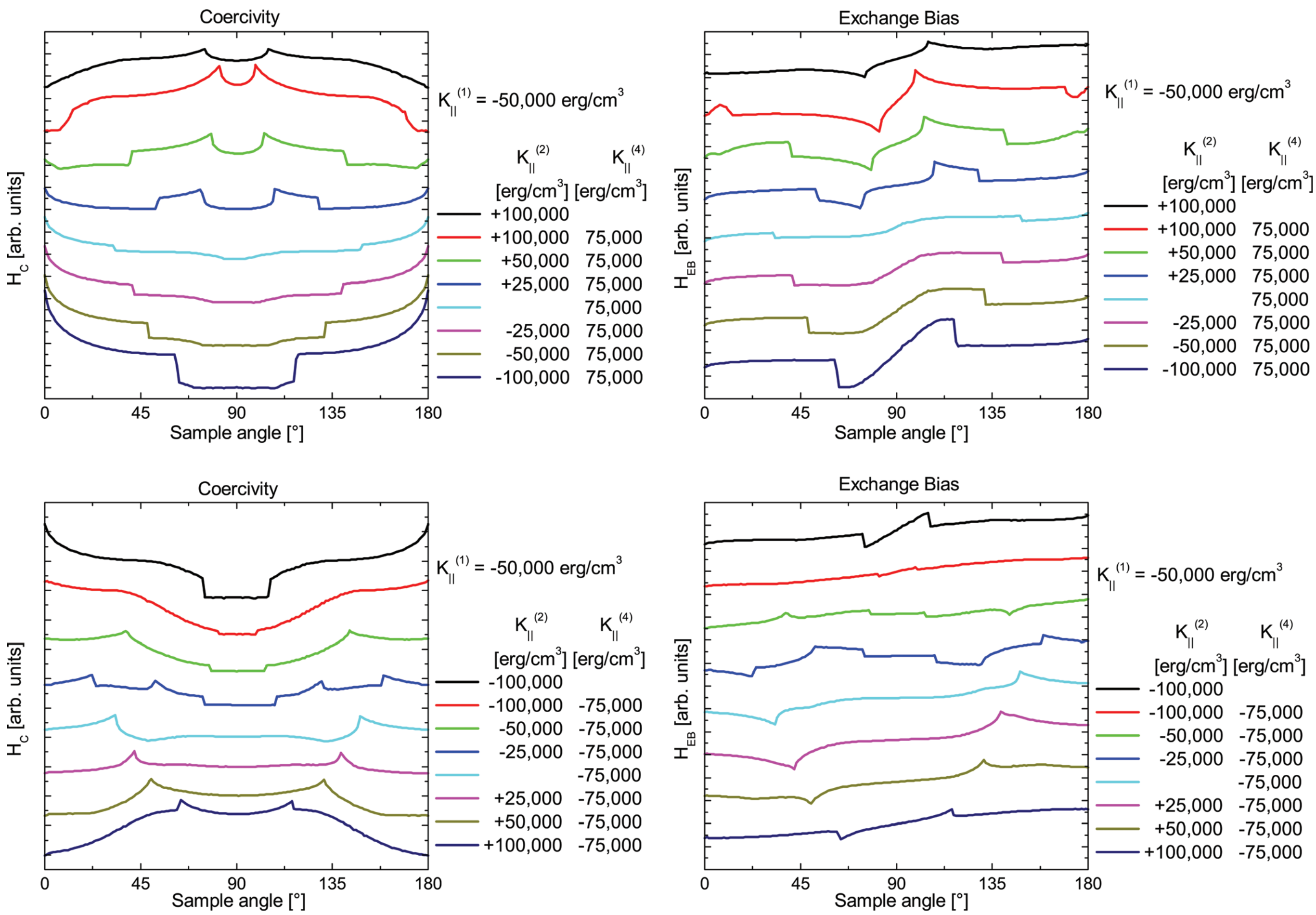

FIG. 2. (Color online) Exchange bias and coercivity, calculated for a series of uniaxial anisotropies $K_{||}^{(2)}$ (lines in the graph are ordered correspondingly to descriptions at the sides), for $K_{||}^{(1)} = -50\ 000$ erg/cm^3 and $K_{||}^{(4)} = -75\ 000$ erg/cm^3 (upper panels)/+ 75 000 erg/cm^3 (lower panels). Lines are vertically shifted for clarity.

state perpendicular to the external field, the longitudinal magnetization component becomes zero, and the coercive field is reached.

A. Split coercivity maxima and rapid changes of exchange bias

We first investigate how the calculated coercivity and exchange bias change for three sets of $K_{||}^{(4)}$ and $K_{||}^{(2)}$, each combined with a series of $K_{||}^{(1)}$ values. While a pure (110) system is assumed to show a constant ratio of $K_{||}^{(4)}$and $K_{||}^{(2)}$,[34] the superposition of the AFM's and the FM's anisotropies may lead to deviations from this case. Especially in the temperature regime not too far below the Néel temperature, experiments can show strong deviations from the characteristics of the high temperature regime—with the pure FM anisotropies—and the low temperature regime, in which the AFM anisotropies dominate.[35] The above chosen values can thus picture different situations of an exchange bias system, appearing at different temperatures. Moreover, they can be used to explore the angle dependence of exchange bias and coercivity theoretically, independent of a real EB system, and thus to develop a feeling for the influences of the different anisotropy constants.

Figure 1 shows the simulated exchange bias H_{EB} and coercivity H_C for $K_{||}^{(4)} = 75\ 000$ erg/cm^3 (i.e., the easy axes are located at 0°, 90°, etc.) and $K_{||}^{(2)} = -25\ 000$ erg/cm^3 (upper panels)/0 (middle panels)/+ 25 000 erg/cm^3 (lower panels). Starting from a small exchange bias (top line in each graph), the coercivity first shows a splitting of the original maximum at 90°, followed by a suppression of this doubled maximum, which vanishes completely with larger values of $K_{||}^{(1)}$. The unidirectional anisotropy which is sufficient to eliminate the maxima around 90° depends strongly on $K_{||}^{(2)}$. For negative values of $K_{||}^{(2)}$, when the easy twofold axis is located at 0°–180°, the hard axis at 90° diminishes the coercivity maximum even without the unidirectional contribution. Consequently, in this case the maximum is completely suppressed for small values of $K_{||}^{(1)}$. However, when $K_{||}^{(2)}$ is positive, i.e. the easy twofold axis is located at 90°–270°, the uniaxial anisotropy strengthens the maximum at 90°. Thus it splits more strongly before it finally vanishes for large values of $K_{||}^{(1)}$.

Similarly, the exchange bias exhibits a qualitatively different angular dependent behavior for different combinations

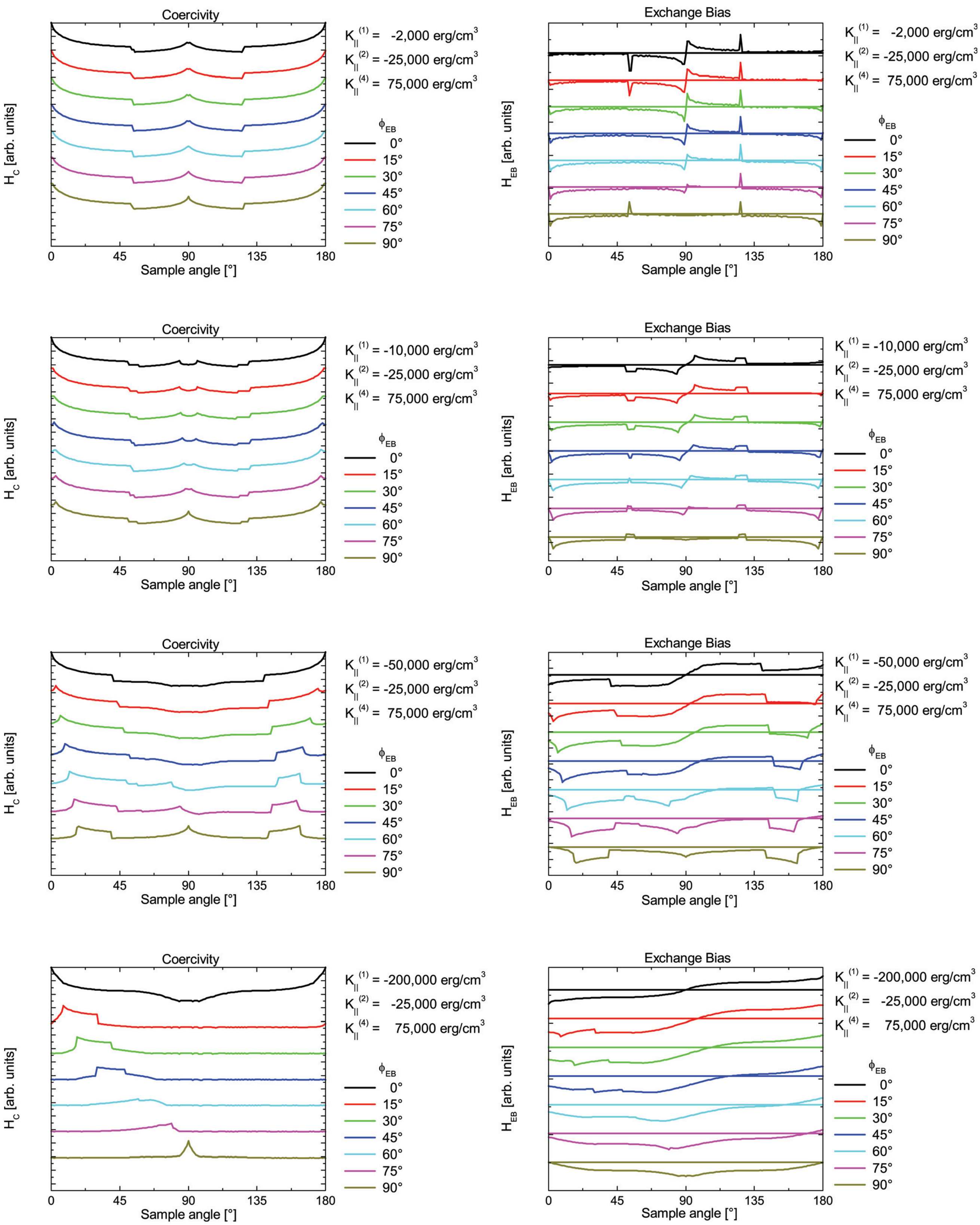

FIG. 3. (Color online) Exchange bias and coercivity, calculated for a series of sample angles (lines in the graph are ordered correspondingly to descriptions at the sides), for $K_{||}^{(2)} = -25\ 000$ erg/cm^3, $K_{||}^{(4)} = +75\ 000$ erg/cm^3, and different unidirectional anisotropies. Lines are vertically shifted for clarity. The lines $H_{EB} = 0$ have been added to each exchange bias graph.

of the three anisotropy constants under examination. The split maximum in the coercivity around 90° is accompanied here by the rapid transition from minimum to maximum values in the form of sharp peaks (one with positive, one with negative sign) in the exchange bias. Both the coercivity and EB characteristic behavior vanish around the same values of the unidirectional anisotropy constants. Steps in the coercivity, as seen in Fig. 1, are also correlated with steps in the exchange bias. It should be mentioned that especially for nonvanishing double-maxima in the coercive field, the exchange bias can reach numerically larger values at angles located off the cooling field direction set to 0°.

In order to examine the influence of the exchange bias direction with respect to the easy fourfold symmetry axis, Fig. 2 shows a comparison of ϕ_{EB} along the easy fourfold axis (upper panels) and the hard fourfold axis (lower panels) for different values of $K_{||}^{(2)}$. The simulation without fourfold anisotropy is added for comparison (top line in each graph).

For field cooling at the easy fourfold axis, the coercivity again shows a qualitatively different behavior, depending on the sign and value of the uniaxial anisotropy. For large positive values of $K_{||}^{(2)}$, the double maximum around 90° is visible, which is suppressed for vanishing or negative values of $K_{||}^{(2)}$. For large negative $K_{||}^{(2)}$, a broad minimum becomes visible around 90°, which is also created for vanishing $K_{||}^{(4)}$ (top line in the lower panel).

If the exchange bias is located along the hard fourfold axis, it exhibits coercive fields with numerous steps; however, the graphs are again strongly influenced by the value of the uniaxial anisotropy constant $K_{||}^{(2)}$. It can be recognized that the double maximum around 90°, which occurs again for large positive $K_{||}^{(2)}$, is now more strongly split, and the peaks are sharper than in the upper panel and do not exhibit similar plateaus.

The exchange bias again shows sharp peaks correlated with the double maximum around 90° as well as the existence of angular regions with significantly enhanced EB values. However, for the EB along the hard fourfold axis (lower panels), there are also regions between 0° and 90° where the exchange bias becomes positive ($H_{EB} = 0$ can be estimated by regarding the EB for a sample angle of 90°, which has to be zero due to symmetry reasons), which is best visible in the curve for $K_{||}^{(2)} = -25\,000$ erg/cm^3 and $K_{||}^{(4)} = -75\,000$ erg/cm^3.

B. Positive exchange bias

A positive exchange bias along the cooling field direction can be found in some magnetic systems, and explanations for this effect have been discussed in literature over the past decades. Since the sign of the exchange bias has been found to depend on the cooling field orientation with respect to the easy AFM axis,[15,36] the simulations have additionally been carried out for several EB angles, combined with $K_{||}^{(2)} = -25\,000$ erg/cm^3, $K_{||}^{(4)} = +75\,000$ erg/cm^3, and different values of the unidirectional anisotropy $K_{||}^{(1)}$. Thus, the exchange bias direction ϕ_{EB} was rotated from 0° (i.e., along the easy twofold and fourfold axes) to 90° (i.e., along the easy fourfold and the hard twofold axes). In Fig. 3, zero lines have been added for each EB graph to allow easier identification of a positive EB behavior.

The coercive fields exhibit unusual features, especially for large exchange bias values. For small $K_{||}^{(1)}$ and ϕ_{EB} near 45° (i.e., the hard fourfold axis), regions with positive EB exist near ϕ_{EB}, as has already been shown in Fig. 2.

Although Fig. 3 does not show any graph with a positive exchange bias along ϕ_{EB}, our study is nevertheless capable of creating a positive EB in the special system under examination without the necessity to take into account microscopic arguments. The energy landscape built by $K_{||}^{(2)} = -25\,000$ erg/cm^3 and $K_{||}^{(4)} = +75\,000$ erg/cm^3, on which the simulations in Fig. 3 are based, has maxima at 55° and 125°, regarding the angular region 0°–180°. If a sample is field cooled at, e.g., 56°, the nearest local energy minimum can be found at ~90°. Thus it is logical to assume that the exchange bias direction ϕ_{EB} created by the field cooling process is *not* 56° but nearly 90°. In this case, for $K_{||}^{(1)} \sim -10\,000$ erg/cm^3 and field cooling at 56°, a positive exchange bias can be expected *in the cooling field direction*, which is assumed here not to be identical with the easy direction of the unidirectional anisotropy ϕ_{EB}. This finding suggests that for experimentally found positive exchange bias values in magnetic systems which are known to show fourfold and uniaxial anisotropies, the samples should be accordingly rotated to test this possibility. On the other hand, our study suggests a possible new way to obtain positive exchange bias and thus to design magnetically biased systems with switchable exchange bias sign for applications which may profit from the positive/negative states of the effect.

III. CONCLUSIONS

In summary, different combinations of fourfold, uniaxial, and unidirectional anisotropies cause angular dependent exchange bias and coercivity values with some characteristic features. A large exchange bias has been shown to suppress a maximum in the coercivity at 90° to the exchange bias direction ϕ_{EB}. Moreover, the exchange bias can become numerically larger at angles different from ϕ_{EB}. On the other hand, in the special system under examination it can reach positive values within the angular region of ±90° around the cooling field direction and even in the cooling field direction which can support trials to develop systems with positive or switchable EB for novel applications.

[1] W. H. Meiklejohn and C. P. Bean, Phys. Rev. **105**, 904 (1957).
[2] J. Nogués and I. K. Schuller, J. Magn. Magn. Mater. **192**, 203 (1999).
[3] A. E. Berkowitz and K. Takano, J. Magn. Magn. Mater. **200**, 552 (1999).
[4] P. Baumgart, B. Hillebrands, and G. Güntherodt, J. Magn. Magn. Mater. **93**, 225-228 (1991).
[5] A. Tillmanns, T. Blachowicz, M. Fraune, G. Güntherodt, and I. K. Schuller, J. Magn. Magn. Mater. **321**, 2932 (2009).
[6] J. Nogués and I. K. Schuller, J. Magn. Magn. Mater. **192**, 203 (1999).
[7] K. G. West, D. N. H. Nam, J. W. Lu, N. D. Bassim, Y. N. Picard, R. M. Stroud, and S. A. Wolf, J. Appl. Phys. **107**, 113915 (2010).
[8] R. P. Singh, C. V. Tomy, and A. K. Grover, Appl. Phys. Lett. **97**, 182505 (2010).
[9] J. Nogués, D. Lederman, T. J. Moran, and I. K. Schuller, Phys. Rev. Lett. **76**, 4624 (1996).
[10] T. M. Hong, Phys. Rev. B **58**, 97 (1998).
[11] H. Ohldag, H. Shi, E. Arenholz, J. Stöhr, and D. Lederman, Phys. Rev. Lett. **96**, 027203 (2006).
[12] J. Nogués, C. Leighton, and I. K. Schuller, Phys. Rev. B **61**, 1315 (2000).
[13] Y. Hu and A. Du, J. Appl. Phys. **102**, 113911 (2007).
[14] W. A. A. Macedo, M. D. Martins, M. J. M. Pires, R. B. Oliveira, C. J. S. M. Pombo, W. C. Nunes, M. Knobel, P. H. O. Rappl, and P. Motisuke, J. Appl. Phys. **102**, 033908 (2007).
[15] X. Y. Xu, H. Y. Tian, X. Quian, and J. G. Hu, J. Appl. Phys. **106**, 093910 (2009).
[16] N. C. Koon, Phys. Rev. Lett. **78**, 4865 (1997).

[17] W. Wang, F. Takano, M. Takenaka, H. Akinaga, and H. Ofuchi, J. Appl. Phys. **103**, 093914 (2008).
[18] T. Gredig, I. N. Krivorotov, P. Eames, and E. D. Dahlberg, Appl. Phys. Lett. **81**, 1270 (2002).
[19] H. C. Choi, C. Y. You, K. Y. Kim, J. S. Lee, J. H. Shim, and D. H. Kim, Phys. Rev. B. **81**, 224410 (2010).
[20] E. Jiménez, J. Camarero, J. Sort, J. Nogués, A. Hoffmann, N. Mikuszeit, J. M. García-Martín, B. Dieny, and R. Miranda, Phys. Rev. B **80**, 014415 (2009).
[21] J. McCord, C. Hamann, R. Schäfer, L. Schultz, and R. Mattheis, Phys. Rev. B **78**, 094419 (2008).
[22] M. O. Liedke, B. Liedke, A. Keller, B. Hillebrands, A. Mücklich, S. Facsko, and J. Fassbender, Phys. Rev. B **75**, 220407(R) (2007).
[23] A. Tillmanns, S. Oertker, B. Beschoten, G. Güntherodt, C. Leighton, I. K. Schuller, and J. Nogués, Appl. Phys. Lett. **89**, 202512 (2006).
[24] C. Leighton, M. R. Fitzsimmons, P. Yashar, A. Hoffmann, J. Nogués, J. Dura, C. F. Majkrzak, and Ivan K. Schuller, Phys. Rev. Lett. **86**, 4394 (2001).
[25] M. R. Fitzsimmons, P. Yashar, C. Leighton, Ivan K. Schuller, J. Nogués, C. F. Majkrzak, and J. A. Dura, Phys. Rev. Lett. **84**, 3986 (2000).
[26] C. Leighton and I. K. Schuller, Phys. Rev. B **63**, 174419 (2001).
[27] I. N. Krivorotov, C. Leighton, J. Nogués, I. K. Schuller, and E. Dan Dahlberg, Phys. Rev. B **65**, 100402(R) (2002).
[28] A. Tillmanns, S. Oertker, B. Beschoten, G. Güntherodt, J. Eisenmenger, and I. K. Schuller, Phys. Rev. B **78**, 012401 (2008)
[29] J. Nogués, D. Lederman, T. J. Moran, I. K. Schuller, and K. V. Rao, Appl. Phys. Lett. **68**, 3186 (1996).
[30] J. Nogués, D. Lederman, T. J. Moran, and I. K. Schuller, Phys. Rev. Lett. **76**, 4624 (1996).
[31] D. Lederman, J. Nogués, and I. K. Schuller, Phys. Rev. B **56**, 2332 (1997).
[32] B. Beckmann, K. D. Usadel, and U. Nowak, Phys. Rev. B **74**, 054431 (2006).
[33] T. Blachowicz, A. Tillmanns, M. Fraune, R. Ghadimi, B. Beschoten, and G. Güntherodt, Phys. Rev. B **75**, 054425 (2007).
[34] B. Hillebrands, Phys. Rev. B **41**, 530 (1990).
[35] A. Tillmanns, Ph.D. thesis, RWTH Aachen University, 2005, http://darwin.bth.rwth-aachen.de/opus3/volltexte/2006/1352/.
[36] E. Jimenez, J. Camarero, J. Sort, J. Nogués, A. Hoffmann, F. J. Teran, P. Perna, J. M. Garcia-Martin, B. Dieny, and R. Miranda, Appl. Phys. Lett. **95**, 122508 (2009).